Title

Complex excitation dynamics underlie polymorphic ventricular tachycardia in a transgenic rabbit model of long QT syndrome type 1.

Journal

Heart Rhythm, 12(1)

Authors

Kim, Tae
Kunitomo, Yukiko
Pfeiffer, Zachary
et al.

Publication Date

2015

DOI

10.1016/j.hrthm.2014.10.003

Peer reviewed

Published in final edited form as:
Heart Rhythm. 2015 January ; 12(1): 220–228. doi:10.1016/j.hrthm.2014.10.003.

Complex excitation dynamics underlie polymorphic ventricular tachycardia in a transgenic rabbit model of long QT syndrome type 1

Tae Yun Kim, PhD[*], **Yukiko Kunitomo, BS**[*], **Zachary Pfeiffer, BS**[*], **Divyang Patel, MD**[†], **Jungmin Hwang, BS**[*,‡], **Kathryn Harrison, MD**[*], **Brijesh Patel, BS**[*], **Paul Jeng, BS**[*], **Ohad Ziv, MD**[§], **Yichun Lu, MS**[*], **Xuwen Peng, DVM, PhD**[¶], **Zhilin Qu, PhD**[‖], **Gideon Koren, MD**[*], and **Bum-Rak Choi, PhD**[*]

[*]Cardiovascular Research Center, Division of Cardiology, Rhode Island Hospital, Warren Alpert Medical School of Brown University, Providence, Rhode Island [†]Cardiovascular Institutes, School of Medicine, University of Pittsburgh, Pittsburgh, Pennsylvania [‡]Department of Pharmacology, University of Rhode Island, Rhode Island [§]Case Western Reserve University, School of Medicine, Cleveland, Ohio [¶]Department of Comparative Medicine, Pennsylvania State University College of Medicine, Hershey, Pennsylvania [‖]Department of Medicine, University of California, Los Angeles, California

Abstract

BACKGROUND—Long QT syndrome type 1 (LQT1) is a congenital disease arising from a loss of function in the slowly activating delayed potassium current I_{Ks}, which causes early afterdepolarizations (EADs) and polymorphic ventricular tachycardia (pVT).

OBJECTIVE—The purpose of this study was to investigate the mechanisms underlying pVT using a transgenic rabbit model of LQT1.

METHODS—Hearts were perfused retrogradely, and action potentials were recorded using a voltage-sensitive dye and CMOS cameras.

RESULTS—Bolus injection of isoproterenol (140 nM) induced pVT initiated by focal excitations from the right ventricle (RV; n = 16 of 18 pVTs). After the pVT was initiated, complex focal excitations occurred in both the RV and the left ventricle, which caused oscillations of the QRS complexes on ECG, consistent with the recent proposal of multiple shifting foci caused by EAD chaos. Moreover, the action potential upstroke in pVT showed a bimodal distribution, demonstrating the coexistence of 2 types of excitation that interacted to produce complex pVT: Na^+ current (I_{Na})-mediated fast conduction and L-type Ca^{2+} current (I_{Ca})-mediated slow conduction coexist, manifesting as pVT. Addition of 2 μM tetrodotoxin to reduce I_{Na} converted pVT into monomorphic VT. Reducing late I_{Na} in computer simulation converted pVT into a single dominant reentry, agreeing with experimental results.

Address reprint requests and correspondence: Dr. Bum-Rak Choi, Cardiovascular Research Center, Rhode Island Hospital and Brown Medical School, Coro West 5101, One Hoppin St, Providence, RI 02903. Bum-Rak_Choi@brown.edu.

CONCLUSION—Our study demonstrates that pVT in LQT1 rabbits is initiated by focal excitations from the RV and is maintained by multiple shifting foci in both ventricles. Moreover, wave conduction in pVT exhibits bi-excitability, that is, fast wavefronts driven by I_{Na} and slow wavefronts driven by I_{Ca} co-exist during pVT.

Keywords

Long QT syndrome; Early afterdepolarization; Ventricular tachycardia; Polymorphic ventricular tachycardia; Action potential duration dispersion; Optical mapping; Bi-excitability

Introduction

Congenital long QT syndrome (LQTS) is a familial disease characterized by prolongation of the QT interval on surface ECG and sudden cardiac death caused by polymorphic ventricular tachycardia (pVT) or “torsades de pointes” (TdP).[1–3] Long QT syndrome type 1 (LQT1) is caused by a mutation in the KCNQ1 gene, which encodes I_{Ks}. The incidence of pVT in LQT1 patients is often associated with sympathetic activation during physical exercise such as swimming. Beta-blocker treatment is more effective in treating LQT1 than other LQTS types (partially effective in LQT2, no benefit in LQT3 patients), suggesting that pVT in LQT1 is highly dependent on sympathetic activation.

The original hypothesis of Dessertenne is that 2 or more foci firing at slightly different frequencies may generate a resonance effect, resulting in the oscillatory ECG pattern.[3] An alternative suggestion is that TdP is caused by a meandering reentrant wave due to prolonged APD and enhanced APD dispersion.[4–6] Optical mapping studies using drug-induced LQT2 animal models have shown that pVT is driven by both meandering waves[7] and multiple foci firing early afterdepolarizations (EADs).[8] However, how multiple foci and their propagation are maintained to form the characteristic TdP pattern in ECG is not clear.

Recent computer modeling studies proposed a bi-excitability hypothesis by which formation and propagation of chaotic EADs can result from 2 excitation fronts driven by sodium (I_{Na}) and L-type Ca^{2+} current (I_{Ca}).[9,10] Lack of repolarization reserve in LQTS may create conditions by which I_{Ca} as well as I_{Na} contribute to excitation and propagation, which allows complex interaction of wavefronts and focal activities to maintain TdP. However, bi-excitability and chaotic excitation have not been demonstrated experimentally in LQTS-related arrhythmias.

The purpose of this study was to investigate the excitation dynamics in LQT1 to better understand the initiation and maintenance mechanisms of pVT. Using a transgenic rabbit model of LQT1, our results reveal that multiple focal activities that shift irregularly in space and time underlie pVT in LQT1 rabbits.[11,12] In addition, we found that I_{Na}-mediated fast conduction and I_{Ca}-mediated slow conduction coexist during pVT, providing the first experimental evidence for bi-excitability and chaotic EAD dynamics in LQT1 rabbits.[9,10]

Methods

Heart preparations

Littermate control (LMC) and transgenic rabbits were injected with buprenorphine (0.03 mg/kg IM), acepromazine (0.5 mg/kg IM), xylazene (15 mg/kg IM), ketamine (60 mg/kg IM), pentothal (35 mg/kg IV), and heparin (200 units/kg). This investigation conforms to the current Guide for Care and Use of Laboratory Animals published by the National Institutes of Health (NIH Publication No. 85-23, revised 1996) and approved by the Lifespan Animal Welfare Committee at Rhode Island Hospital. The heart was excised from the chest and retrogradely perfused through the aorta with the following (in mmol/L): 130 NaCl, 24 $NaHCO_3$, 1.0 $MgCl_2$, 4.0 KCl, 1.2 NaH_2PO_4, 5 dextrose, 25 mannitol, and 1.25 $CaCl_2$, at pH 7.4, and gassed with 95% O_2 and 5% CO_2. Eighteen rabbits were studied: 13 LQT1 (9 male and 4 female) and 5 LMC (3 male and 2 female) weighing 3.9 ± 0.6 kg and aged 9 ± 3 months. Hearts were placed in a water-heated chamber to maintain temperature at 37.0° ± 0.2°C. Blebbistatin (5 μmol/L) was added to reduce movement artifact.

Optical mapping

The optical apparatus has been previously described.[13] Fluorescence images from the anterior and posterior surfaces of the heart were captured using 2 CMOS cameras (100 × 100 pixels, Ultima-L, Scimedia, Japan), which results in a field of view of 2 × 2 cm^2. Hearts were stained with the voltage-sensitive dye di-4 ANEPPS (Invitrogen, Carlsbad, CA) by delivering 25 μL of stock solution (1 mg/mL in dimethyl sulfoxide) through a bubble trap above the aortic cannula.

Sequence of experiment

Figure 1 shows the sequence of our experimental protocol. Once hearts were stabilized in the perfusion system, the right atrium was opened and the AV node ablated with a cautery system (Thermal Cautery Unit, Geiger). AV ablation slowed the heart rate (typical cycle length [CL] 700–1000 ms). If the heart rate dropped below 30 bpm (CL >2000 ms), the heart was paced at 2000-ms CL. Isoproterenol was delivered as a bolus injection into the bubble trap (5 mL, 140 nM) to AV-ablated hearts to trigger pVT in LQT1 hearts. LMC hearts (n = 5) did not demonstrate EADs or pVT under the same conditions. LQT1 hearts were then perfused for 20 minutes with 2 μM tetrodotoxin (TTX) to partially block I_{Na}.

Data analysis

Activation and repolarization—The activation and repolarization time-points at each pixel were determined from fluorescence (F) signals by calculating $(dF/dt)_{max}$ and $(d^2F/dt^2)_{max}$. APD dispersion was defined as the difference between maximum and minimum APD ($\Delta APD_{|max-min|}$) across the field of view.[13] The rate of rise (upstroke velocity) was calculated from each action potential by $[dV/dt]_{max}$. Because fluorescence signal is not truly transmembrane potential (V_m), we normalized fluorescence traces to the first full action potential during the initiation of pVT.

Detection of foci in pVT—Waves appearing in the field of view were automatically detected as follows. Five consecutive images were checked (including the 2 previous and 2

following frames) to reduce false detection of new waves due to background noise. Only new waves that appeared within the field of view were identified, of which the waves with increasing area in the following frame from concentric activation were considered foci (Figure 1B).

Computer simulation

Computer simulations were carried out in a simplified cylindrical tissue model (300 × 300 cells). The action potential model was modified to include late Na^+ current (I_{NaL}) from the rabbit myocyte model to induce EADs.[14] Detailed parameter set and modifications are described in the Online Supplementary Material.

Statistical analysis

Normally distributed variables were compared using a Student unpaired *t* test. The Otsu thresholding method was applied to separate bimodal distribution of $[dV/dt]_{max}$ by minimizing the intraclass variance.[15] The point pattern of foci was analyzed using the average nearest neighbor (ANN) ratio.[16] This algorithm calculates the average distance between a focal site and its nearest neighbor and compares it to the expected value of a random/uniform distribution within the same parameters. An ANN ratio of 1 means that the point pattern of foci is random, whereas ANN <1 means the interfoci distance is smaller and the foci are clustered.

Results

Increased APD dispersion associated with pVT induction

We previously reported that at basic CL of 350 ms, APD dispersion in LQT1 rabbits was similar to that of LMCs but significantly smaller than that of LQT2 rabbits.[11] Here we examined the rate-dependent dynamics of APD dispersion in LQT1 at slower heart rates. Sample traces from the right ventricle (RV) and left ventricle (LV) suggest that APD dispersion increases between RV and LV at slow heart rates (Figure 2A). Sample APD maps at 350- and 2000-ms CL show increasing APD dispersion from 17.3 ± 2.9 ms to 39.8 ± 7.5 ms (n = 7; Figure 2B).

Bolus injection of isoproterenol induced pVT in LQT1 hearts (9 of 10) but elicited neither pVT nor ventricular fibrillation in any of the 5 LMC hearts. The first beat of pVT in LQT1 generally arose from the anterior region of the RV. Figure 3 shows an example of simultaneous recordings from the anterior and posterior regions using dual CMOS cameras. Interestingly, the first action potential in the RV repolarized (marked as ① in Figure 3A) and fired an additional action potential that initiated pVT (marked as ② in Figure 3A), whereas the LV was still in the plateau phase. Of the 18 pVTs, 16 (88%) were initiated from the RV.

Shifting foci underlie undulating ECG pattern in pVT

It is generally thought that pVTs in LQTS are triggered by EADs, but the role of EADs in maintaining pVT is not clearly understood. We investigated activation patterns to determine whether EADs induce reentry to maintain pVT in LQT1 rabbits. The series of maps in

Figure 4 shows a typical ECG and corresponding activation maps of pVT. The numerous concentric activations in pVT indicate that, in addition to initiation, focal activity contributes to pVT maintenance by generating new waves (Figure 4). During the early phase of pVT (marked in green in Figure 4A), focal activities in the posterior region dominated activation patterns. However, after 2 seconds, the focal activities moved to the anterior region (yellow box in the trace panel and activation maps in the bottom panel).

On average, 13 foci were observed per second, and 31% ± 5% of the individual waves originated from focal activity (n = 18 pVT episodes). Although most pVTs were initiated from the RV, cumulative foci plots suggest that focal activity is widely distributed across the entire anterior region of the hearts, including the RV and LV (Figure 4B). The average distance between 1 focal site and the next was 6.5 ± 0.5 mm (11 pVT episodes), which indicates that focal activity is not completely random but rather moves to the proximity of the previous focal site, as shown by the activation maps in Figure 4B.

Two distinct types of action potential upstrokes in pVT

Computer modeling studies suggest that EADs and their propagation can be influenced by both I_{Ca} and I_{Na} in LQTS.[9,10] We hypothesized that if pVT of LQT1 hearts is maintained by both I_{Ca}- and I_{Na}-mediated excitation wavefronts, the action potentials of pVT will show rapid and slow-rising upstrokes that correspond to I_{Na}- and I_{Ca}-mediated excitations, respectively. We calculated the first derivatives of voltage traces during pVT (Figure 5A) and found 3 distinct patterns in the histograms (Figure 5B): fast upstroke (a), slow upstroke (b), and 2 peaks of both fast and slow upstrokes (Figure 5C). Panel B shows a probability density plot of $[dV/dt]_{max}$ of all the excitation waves in Figure 5A. Overall, few action potentials were driven by the fast upstroke (5% ± 0.3%). In addition, the sites of focal activity have a lower range of $[dV/dt]_{max}$ and higher V_m (Figure 5C), indicating that focal activity is mainly driven by I_{Ca}.

TTX reduces EADs and converts pVT to monomorphic VT (mVT)

We further investigated whether I_{Na} is an essential depolarizing current for EADs and maintaining pVT in LQT1 with the I_{Na} blocker TTX. At 2 μM (IC_{50} = 1.5 μM for late I_{Na} current), TTX converted pVTs into monomorphic ventricular tachycardia (mVT) and prevented EAD formation (4 of 4 hearts).[17] Figure 6 illustrates the transition to mVT. The arrhythmia began with pVT with multiple focal activity (green box in Figure 6A and maps of ②–④), then multiple focal activity gradually disappeared as a repetitive activation pattern from apex became dominant in mVT transition (red box and maps of ⑥–⑧). The histograms and maps of $[dV/dt]_{max}$ (Figures 6C and 6D) show a transition from the combination of slow and fast action potential upstrokes toward a fast upstroke, indicating that mVT is maintained by I_{Na}-mediated excitation waves. Average nearest-neighbor analysis (see Methods) revealed that the transition from pVT to mVT involves a reduction in distance between foci (ratio from 0.91 ± 0.06 to 0.65 ± 0.16, $P < .05$), which implies that multifocal activity was markedly reduced by TTX. Another I_{NaL} blocker, ranolazine, also produced mVT with a single rotor formation (see Online Supplementary Figure 6). These results support I_{Na} as an important contributor to the generation of EADs and their propagations.

Reducing I_{Na} and I_{NaL} in computer simulation creates stable reentry

We examined whether the previous computer model of pVT produces bimodal distribution of action potential upstroke due to I_{Na} and I_{Ca}-mediated excitation waves.[14] During pVT, V_m, and upstroke (dV/dt), the maps in Figure 7 show 2 different excitation waves: fast upstroke excitation wave pattern matches the I_{Na} map, whereas slow upstroke matches the I_{Ca} map, in line with our experimental results presented in Figure 5. Further reduction in I_{Na} (25%) and I_{NaL} (100%) reduced multifocal activity and caused stable reentry formation (Figure 7B), similar to the experimental result with TTX in Figure 6. Depending on the initial conditions, a rotor can be formed and anchor in the middle region (Figure 7B, top), similar to the experimental results with ranolazine (see Online Supplementary Figure 6). If a rotor forms near the boundary, it can move out of the boundary, which leaves a rotating wave around the cylinder (Figure 7, bottom). The upstroke distribution in both cases shows transition to fast upstroke, meaning I_{Na}-mediated excitation. This computer simulation further supports the contention that reducing I_{Na} changes pVT into more stable reentry.

Discussion

EADs are the hallmark of LQTS, in which they are generally believed to trigger pVT. However, questions remain whether EADs play additional roles in maintaining complex waveforms in pVT. In this study, we found the following: (1) pVT in LQT1 rabbits is initiated by focal excitations, mainly originating from the RV; (2) multifocal excitations during pVT exhibit no preferred locations, in agreement with computer modeling studies showing multiple shifting foci as a result of dynamical chaos[10]; (3) upstroke velocity exhibits a bimodal distribution, indicating the coexistence of I_{Na}- and I_{Ca}-mediated excitation wavefronts, in line with a novel theory of bi-excitability[9]; and (4) partially blocking I_{Na} using 2 μM TTX reduced focal activity and converted pVT to mVT.

RV origin of pVT in LQT1 rabbits

Slowing of the heart rate by AV ablation also increased APD dispersion between RV and LV (Figure 2). Importantly, most pVT initiated from the RV. Enhanced APD dispersion and pVT initiation from RV may be due to the heterogeneity in I_{to} between RV and LV. I_{to} has been reported to have higher density in the RV,[18] and it can provide a strong repolarizing current and shorten APD.[14,19] Because of the limitation of optical mapping in which fluorescence recording is the sum of multiple cells, it is difficult to recognize potential differences of action potential notch between RV and LV, and single-cell voltage-clamp study is needed to verify the role of I_{to} and its heterogeneity in LQT1 rabbits. Interestingly, the first triggered action potentials in RV tend to occur at the late stage of the repolarization (Figures 2–5). Burashnikov and Antzelevitch[20] demonstrated that delayed afterdepolarizations rather than EADs were frequently observed in a drug-induced animal model of LQT1. It is possible that the first triggered beats originating from RV in LQT1 rabbit hearts are excitations caused by delayed afterdepolarizations or EADs originating from tissue under the epicardial surface. Further studies are needed to determine the role of I_{to} in APD dispersion and pVT initiation mechanisms in LQT1 rabbits.

Dynamics of multiple foci in pVT

The multifocal hypothesis by Dessertenne states that 2 or more foci fire at slightly different frequencies, which gives rise to the ECG morphology of TdP. Our mapping results suggest that during pVT in LQT1, focal activities are not fixed in space but vary dynamically and irregularly, spanning the whole heart. It is notable that most pVT in our LQT1 hearts spontaneously terminated after focal activities stopped (only n = 1 pVT transitioned to ventricular fibrillation of 18 pVT). A study of the mechanisms of multiple shifting foci by Sato et al[10] showed that regional synchronization of chaotic EADs caused dynamically shifting foci, which also may be responsible for the results shown in Figure 4.

The average distance between 1 focal site and the next focal site was 6.5 mm, much shorter than what the average distance should be for completely random events (10 mm in our 20 × 20 mm^2 field of view). This analysis supports the shifting foci hypothesis, by which an EAD, once formed, travels only a short distance and triggers subsequent EADs in neighboring regions. Alternatively, the source–sink relationship between EAD firing cells vs neighboring cells may limit the possible sites of EADs.[21]

Bi-excitability in LQT1 rabbits

Bi-excitability is an extension of bi-stability (2 stable states), a widely recognized phenomenon in nonlinear dynamics that has been demonstrated in many biologic systems. The term bi-excitability was coined to describe 2 excitable states in cardiac tissue. It predicts that I_{CaL} alone can form a regenerative depolarization during the plateau phase of action potential and allow propagation when the repolarization reserve is reduced.[9,10] This theory also predicts that 2 excitation fronts driven by I_{Na} and I_{CaL} can interact and form complex excitation waves such as in pVT. EADs in most cases arise from I_{CaL} reactivation, but whether I_{CaL}-driven EADs can propagate without triggering I_{Na}-driven action potentials was not known.[22,23] Our experimental and computer modeling, particularly $[dV/dt]_{max}$ histograms, showed 2 distinct peaks, demonstrating I_{Na}- and I_{Ca}-driven depolarizations. Perturbation of tissue bi-excitability by TTX dramatically changed excitation dynamics, supporting the contention that bi-excitability underlies complex waves of pVT in LQT1 rabbits.

I_{Na} and maintenance of pVT

It is surprising that reducing I_{Na} caused transition to mVT both in our experiment (Figure 6) and in computer simulation (Figure 7). The transition to mVT includes a decrease in multiple focal activity. EADs are generally thought to be generated by reactivation of L-type Ca^{2+} current ($I_{Ca,L}$) and/or Na^+/Ca^{2+} exchanger (I_{NCX}) via spontaneous Ca^{2+} release. However, there is increasing evidence that late sodium current (I_{NaL}) also may contribute to EAD formation. Several groups reported that ranolazine, an I_{NaL} blocker, suppresses EAD formation in drug-induced LQTS animal models, ischemia/reperfusion-induced arrhythmias, and heart failure.[24–26] We used 2 μM TTX, a concentration known to block most I_{NaL} (IC_{50} = 1.5 μM) with minimal effect on peak I_{Na}.[17] Ranolazine at 10 μM showed similar results. The reduction in the number and possible sites of focal activity by TTX and ranolazine (see Online Supplementary Figure 6) suggest that I_{NaL} provides additional depolarizing currents

during the plateau phase of action potentials and promotes complex EAD dynamics in LQT1.

Study limitations

LQT1 rabbit hearts demonstrated pVT after AV ablation, as described in the Methods. However, the reason why AV ablation in LQT1 rabbits is required for pVT initiation is not clear. A potential explanation is that rabbit heart rates are relatively fast compared to human heart rates. The typical CL preceding pVT in LQT1 rabbits was in the 700-ms range after AV ablation (see Online Supplementary Figures 4 and 5), which is not far from the accelerated heart rate during pVT initiation in LQT1 patients.[27] Recent clinical studies strongly suggest that the high-risk subgroup of LQT1 patients tend to show significant reduction in heart rate after exercise compared to the low-risk subgroup.[28] Further studies are needed to determine whether a reduction in heart rate is sufficient and how vagal activation is involved in LQT1 pVT.

Conclusion

Using a transgenic rabbit model of LQT1, we found that pVT is preferentially initiated from the RV and maintained by multiple shifting foci, which underlies the undulating QRS pattern of TdP. The complex nature of pVT was due to the contributions of both I_{Na} and I_{Ca} and their propagation under existing tissue heterogeneities between RV and LV. Our study emphasizes the role of I_{NaL} in pVT in LQT1 and provides direct evidence of the recently proposed bi-excitability hypothesis, that is, the coexistence of 2 types of excitations mediated by I_{Na} and/or I_{CaL} that promote complex excitation patterns and maintain pVT in the transgenic rabbit model of LQT1.

Supplementary Material

Refer to Web version on PubMed Central for supplementary material.

Acknowledgments

This work was supported by National Heart, Lung, and Blood Institute Grant R01-HL-096669-04 to Dr. Choi and Grants R01-HL-046005-18A1 and R01 HL110791-01A1 to Dr. Koren.

ABBREVIATIONS

ANN	average nearest neighbor
APD	Action potential duration
CL	cycle length
EAD	early afterdepolarization
LMC	littermate control
LQT1	long QT syndrome type 1
LQTS	long QT syndrome

LV	left ventricle
mVT	monomorphic ventricular tachycardia
pVT	polymorphic ventricular tachycardia
RV	right ventricle
TdP	torsades de pointes
TTX	tetrodotoxin
V_m	transmembrane potential
VT	ventricular tachycardia

References

1. Saenen JB, Vrints CJ. Molecular aspects of the congenital and acquired long QT syndrome: clinical implications. J Mol Cell Cardiol. 2008; 44:633–646. [PubMed: 18336833]
2. Schwartz PJ. The congenital long QT syndromes from genotype to phenotype: clinical implications. J Intern Med. 2006; 259:39–47. [PubMed: 16336512]
3. Dessertenne F. La tachycardie ventricularire à deux foyers opposés variables. Arch Mal Coeur. 1966; 59:263–272. [PubMed: 4956181]
4. Starmer CF, Romashko DN, Reddy RS, Zilberter YI, Starobin J, Grant AO, Krinsky VI. Proarrhythmic response to potassium channel blockade: numerical studies of polymorphic tachyarrhythmias. Circulation. 1995; 92:595–605. [PubMed: 7634474]
5. Abildskov JA, Lux RL. Simulated torsade de pointes: the role of conduction defects and mechanism of QRS rotation. J Electrocardiol. 2000; 33:55–64. [PubMed: 10691175]
6. Abildskov JA, Lux RL. Cycle-length effects on the initiation of simulated torsade de pointes. J Electrocardiol. 1994; 27:1–9. [PubMed: 8120472]
7. Gray RA, Jalife J, Panfilov A, Baxter WT, Cabo C, Davidenko JM, Pertsov AM. Nonstationary vortexlike reentrant activity as a mechanism of polymorphic ventricular tachycardia in the isolated rabbit heart. Circulation. 1995; 91:2454–2469. [PubMed: 7729033]
8. Choi BR, Burton F, Salama G. Cytosolic Ca^{2+} triggers early afterdepolarizations and torsade de pointes in rabbit hearts with type 2 long QT syndrome. J Physiol. 2002; 543:615–631. [PubMed: 12205194]
9. Chang MG, Sato D, de Lange E, Lee JH, Karagueuzian HS, Garfinkel A, Weiss JN, Qu Z. Bi-stable wave propagation and early afterdepolarization-mediated cardiac arrhythmias. Heart Rhythm. 2012; 9:115–122. [PubMed: 21855520]
10. Sato D, Xie LH, Sovari AA, Tran DX, Morita N, Xie F, Karagueuzian H, Garfinkel A, Weiss JN, Qu Z. Synchronization of chaotic early afterdepolarizations in the genesis of cardiac arrhythmias. Proc Natl Acad Sci U S A. 2009; 106:2983–2988. [PubMed: 19218447]
11. Brunner M, Peng X, Liu GX, et al. Mechanisms of cardiac arrhythmias and sudden death in transgenic rabbits with long QT syndrome. J Clin Invest. 2008; 118:2246–2259. [PubMed: 18464931]
12. Gravelin, L.; Ziv, O.; Liu, G.; Hartmann, K.; Patel, D.; Schofield, L.; Chaves, L.; Shearer, M.; Koren, G.; Choi, B. Transgenic LQT1 animal model reveals shifiting focus of EADs as mechanism for polymorphic ventricular tachycardia. Poster presented at the 33rd Annual Scientifc Sessions of the Heart Rhythm Society; May 9–12, 2012; Denver, Colorado. p. PO3-104
13. Choi BR, Jang W, Salama G. Spatially discordant voltage alternans cause wavebreaks in ventricular fibrillation. Heart Rhythm. 2007; 4:1057–1068. [PubMed: 17675081]
14. Zhao Z, Xie Y, Wen H, Xiao D, Allen C, Fefelova N, Dun W, Boyden PA, Qu Z, Xie LH. Role of the transient outward potassium current in the genesis of early afterdepolarizations in cardiac cells. Cardiovasc Res. 2012; 95:308–316. [PubMed: 22660482]

15. Otsu N. A threshold selection method from gray-level histograms. IEEE Trans sys Man Cyber. 1979; 9:62–66.
16. Mitchell, A. The ESRI Guide to GIS Analysis Volume 1: Geographic Patterns & Relationships. ESRI Press; 2005.
17. Maltsev VA, Sabbah HN, Higgins RS, Silverman N, Lesch M, Undrovinas AI. Novel ultraslow inactivating sodium current in human ventricular cardiomyocytes. Circulation. 1998; 98:2545–2552. [PubMed: 9843461]
18. Rosati B, Grau F, Rodriguez S, Li H, Nerbonne JM, McKinnon D. Concordant expression of KChIP2 mRNA, protein and transient outward current throughout the canine ventricle. J Physiol. 2003; 548:815–822. [PubMed: 12598586]
19. Bassani RA, Altamirano J, Puglisi JL, Bers DM. Action potential duration determines sarcoplasmic reticulum Ca^{2+} reloading in mammalian ventricular myocytes. J Physiol. 2004; 559:593–609. [PubMed: 15243136]
20. Burashnikov A, Antzelevitch C. Acceleration-induced action potential prolongation and early afterdepolarizations. J Cardiovasc Electrophysiol. 1998; 9:934–948. [PubMed: 9786074]
21. Xie Y, Sato D, Garfinkel A, Qu Z, Weiss JN. So little source, so much sink: requirements for afterdepolarizations to propagate in tissue. Biophys J. 2010; 99:1408–1415. [PubMed: 20816052]
22. January CT, Riddle JM. Early afterdepolarizations: mechanism of induction and block: a role for L-type Ca^{2+} current. Circ Res. 1989; 64:977–990. [PubMed: 2468430]
23. January CT, Riddle JM, Salata JJ. A model for early afterdepolarizations: induction with the Ca^{2+} channel agonist Bay K 8644. Circ Res. 1988; 62:563–571. [PubMed: 2449297]
24. Belardinelli L, Shryock JC, Fraser H. Inhibition of the late sodium current as a potential cardioprotective principle: effects of the late sodium current inhibitor ranolazine. Heart. 2006; 92(Suppl 4):iv6–iv14. [PubMed: 16775092]
25. Fraser H, Belardinelli L, Wang L, Light PE, McVeigh JJ, Clanachan AS. Ranolazine decreases diastolic calcium accumulation caused by ATX-II or ischemia in rat hearts. J Mol Cell Cardiol. 2006; 41:1031–1038. [PubMed: 17027025]
26. Undrovinas AI, Belardinelli L, Undrovinas NA, Sabbah HN. Ranolazine improves abnormal repolarization and contraction in left ventricular myocytes of dogs with heart failure by inhibiting late sodium current. J Cardiovasc Electrophysiol. 2006; 17(Suppl 1):S169–S177. [PubMed: 16686675]
27. Tan HL, Bardai A, Shimizu W, Moss AJ, Schulze-Bahr E, Noda T, Wilde AA. Genotype-specific onset of arrhythmias in congenital long-QT syndrome: possible therapy implications. Circulation. 2006; 114:2096–2103. [PubMed: 17088455]
28. Crotti L, Spazzolini C, Porretta AP, et al. Vagal reflexes following an exercise stress test: a simple clinical tool for gene-specific risk stratification in the long QT syndrome. J Am Coll Cardiol. 2012; 60:2515–2524. [PubMed: 23158531]

Appendix. Supplementary data

Supplementary data associated with this article can be found in the online version at http://dx.doi.org/10.1016/j.hrthm.2014.10.003.

CLINICAL PERSPECTIVES

Long QT syndrome is a heritable disease associated with malignant arrhythmias and sudden cardiac death. We discovered that the transgenic rabbit model of long QT syndrome type 1 develops polymorphic ventricular tachycardias (VTs) similar to humans and that these VTs are maintained by multiple focal activities rather than reentry alone, and that excitation waves that underlie the arrhythmias are either I_{Na}-mediated or I_{Ca}-mediated, a novel conduction behavior during arrhythmias. These waves create a complex excitation dynamics that cause the phenomena of polymorphic VTs. We posit that targeting bi-excitability could lead to new therapeutic approaches for sudden cardiac death in long QT syndrome. For example, late sodium channel blocker could be tested to reduce arrhythmia risk in long QT syndrome.

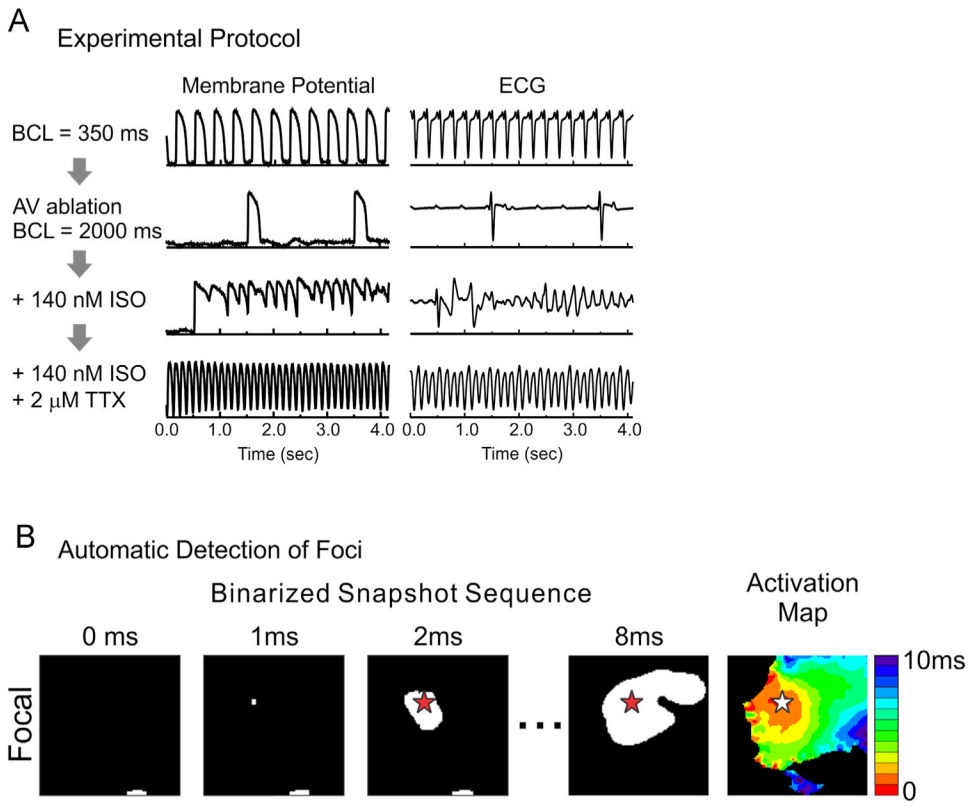

Figure 1.

Experimental procedure and automatic foci detection. **A:** Sequence of the experimental protocol for optical mapping of long QT syndrome type 1 hearts. Sample membrane potential traces from each step are shown at **right. B:** Automatic foci detection. A concentric activation appearing in the field of view was considered a focal site. The corresponding activation maps are shown in the **right.** AV = atrioventricular; BCL = basic cycle length; ISO = isoproterenol; TTX = tetrodotoxin.

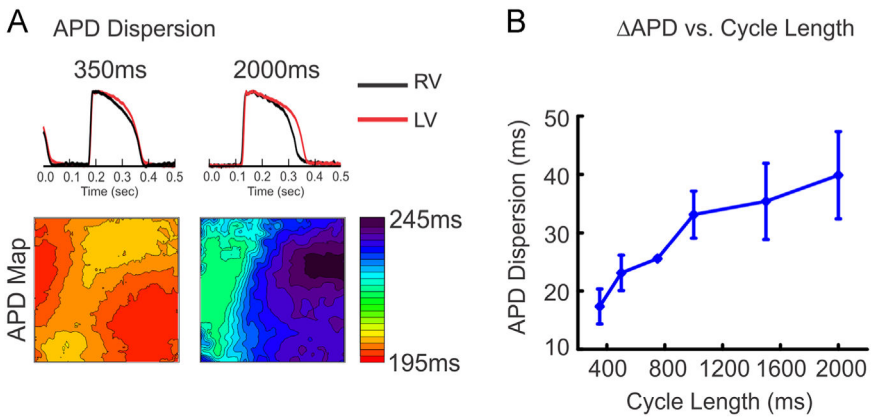

Figure 2.

Rate-dependent action potential duration (APD) dispersion in long QT syndrome type 1. A: APD maps at cycle length (CL) = 350 ms and 2000 ms. Dispersion increases at a slower rate mostly between right ventricle (RV) vs left ventricle (LV). **B:** ΔAPD vs CL, showing that APD dispersion systematically increases with prolonged CL ($\Delta APD_{max-min}$ = 17.3 ± 23.0 msec at 350-ms CL and 40.9 ± 7.4 ms at 2000-ms CL, n = 7).

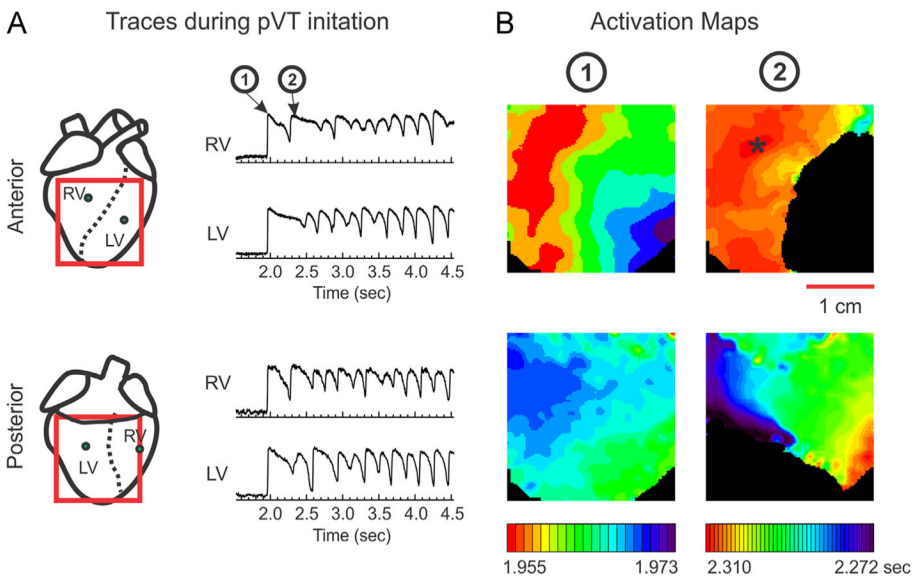

Figure 3.

Initiation of polymorphic ventricular tachycardia (pVT) from the right ventricle (RV). **A:** Sample traces from RV and left ventricle (LV) during initiation of pVT. Note that the first action potential repolarizes in the RV, whereas the same action potential in LV is still in the plateau phase. **B:** Activation maps of the first and second beats marked in panel **A.** The first triggered activity (②) originated in the region of RV (n = 16 of 18 pVTs) and was blocked in the anterior region of LV, but propagated to the anterior apex **(top)** and posterior LV **(bottom).**

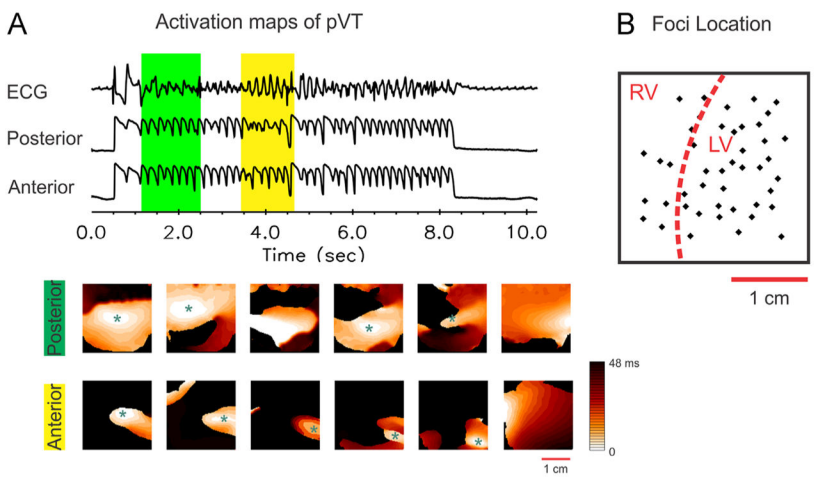

Figure 4.

Multiple focal activities during polymorphic ventricular tachycardia (pVT). **A:** Sample traces and activation maps during pVT. The series of activation maps is shown in the **bottom** panel. The posterior region showed multiple focal activity during the early phase of pVT (*green shading* in trace panel and top activation maps), but focal activity later appeared in the anterior region of left ventricle (LV) and moved toward the apical region (lower activation maps). No meandering spiral was observed. **B:** Spatial distribution of foci during pVT. RV = right ventricle.

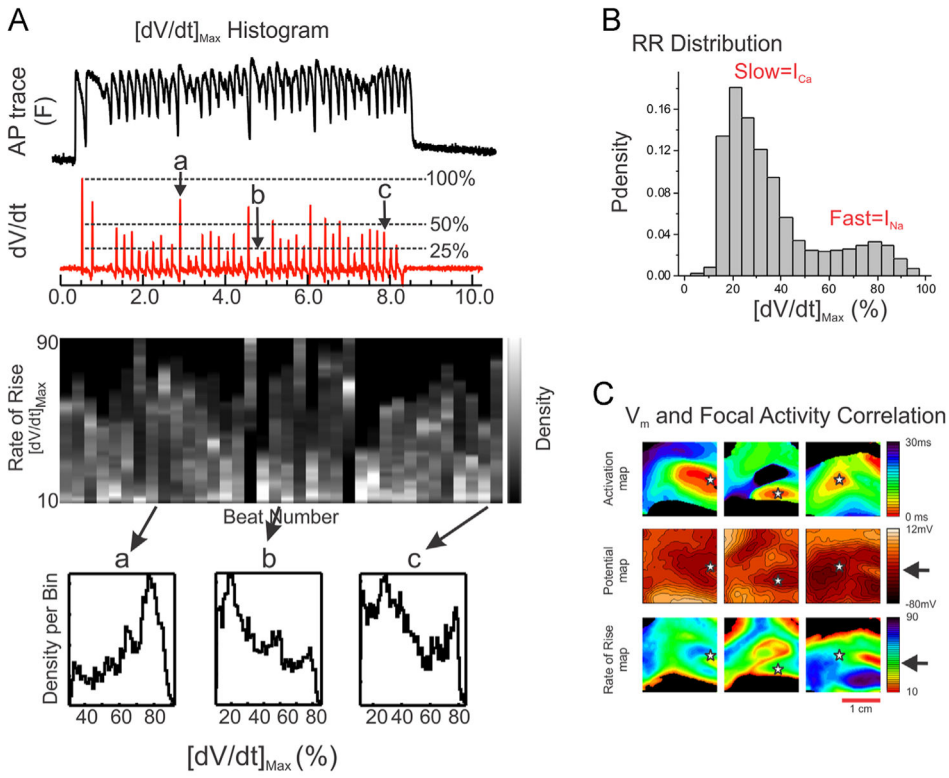

Figure 5.

Bimodal distribution of action potential upstrokes in polymorphic ventricular tachycardia (pVT). **A:** Histograms of $[dV/dt]_{max}$. A sample action potential trace and its first derivatives *(red)* are shown in the **top** panel. Histograms of $[dV/dt]_{max}$ from each action potential are shown in *gray*. Three sample histograms are shown in the **bottom** panel: rapid rise (a), slow rise (b), and both slow and rapid rise (c). **B:** Cumulative distribution of $[dV/dt]_{max}$ supports 2 distinct populations, suggesting the existence of both I_{Na}- & I_{Ca}-mediated excitation wavefronts in pVT. **C:** $[dV/dt]_{max}$ at the site of focal activity. **Left:** Maps of $[dV/dt]_{max}$ and takeoff potential of focal activity (marked by *stars).* **Right:** Histogram of $[dV/dt]_{max}$ from 266 focal activations. Mean value of $[dV/dt]_{max}$ was 23.5% ± 12.3%, suggesting the important role of I_{Ca} in initiating focal activity.

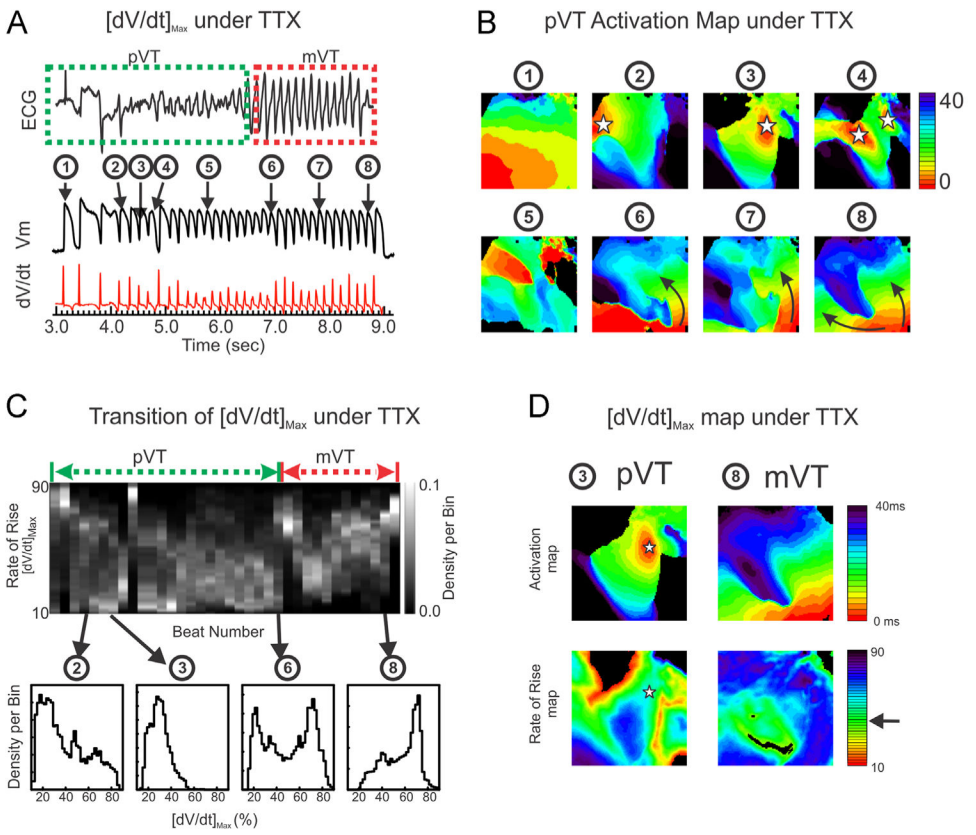

Figure 6.

Blocking I_{Na} with tetrodotoxin (TTX) changes polymorphic ventricular tachycardia (pVT) to monomorphic ventricular tachycardia (mVT). **A:** ECG and V_m traces after 2 μM TTX. Isoproterenol induced pVT (section in *green box)* but then transformed to mVT (section in *red box).* **B:** Series of activation maps during transition to mVT. Focal activity progressively diminished, and repetitive patterns appeared during mVT. **C:** Compiled histograms show a shift to higher $[dV/dt]_{max}$ during the mVT phase. **D:** $[dV/dt]_{max}$ maps from pVT and mVT beats. *Arrow* in the color bar indicates the level of $[dV/dt]_{max}$ at the foci marked with a *star*. Unlike pVT, the map of $[dV/dt]_{max}$ from mVT showed fast action potential upstrokes, indicating that I_{Na}-mediated excitation maintains mVT after TTX.

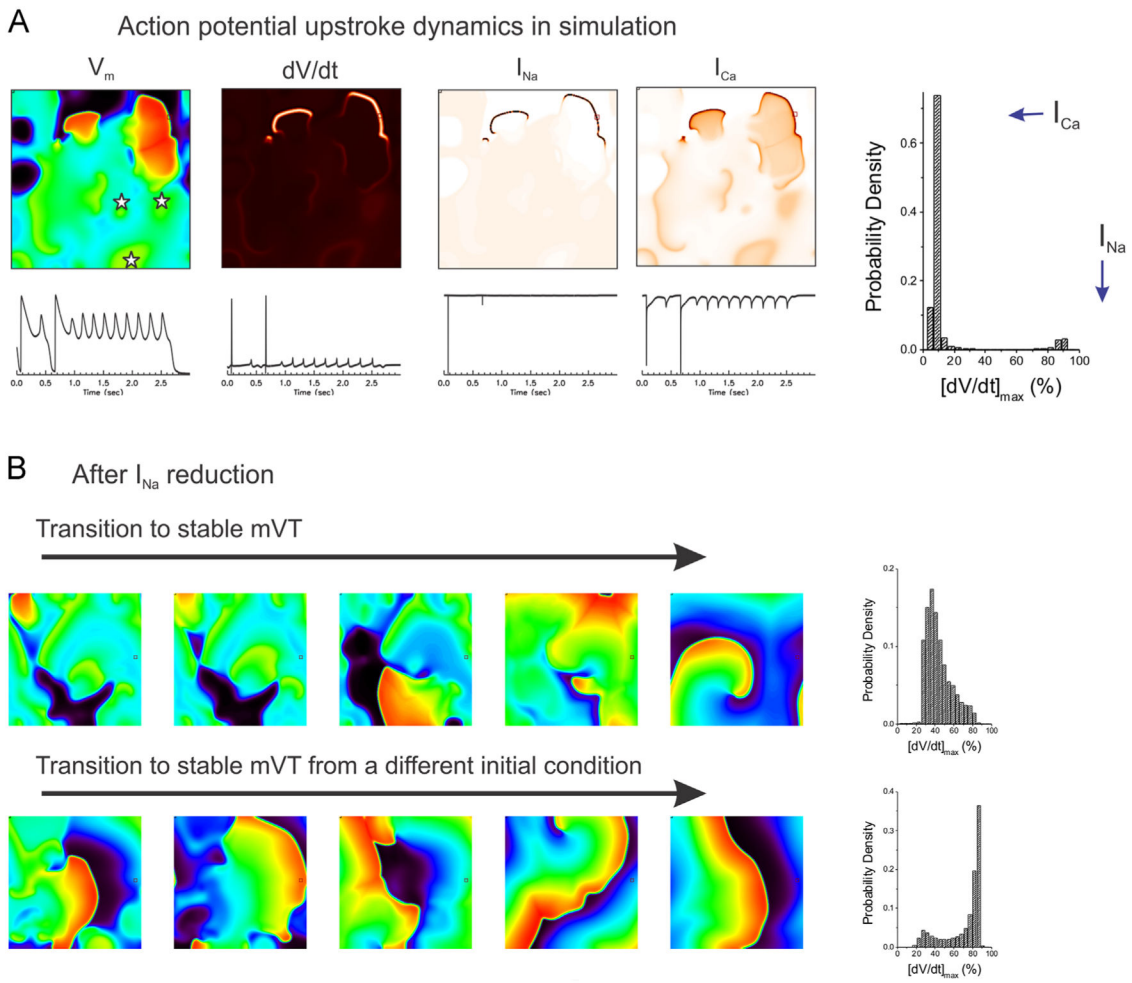

Figure 7.

Computer modeling of tetrodotoxin effect on waves. **A:** Snapshots of $V_{m,}$ dV/dt, I_{Na}, and I_{Ca}. Two distinct upstroke velocities of excitation waves in the dV/dt map correspond to I_{Na} and $I_{Ca,}$ respectively. The histogram of upstroke velocities shows bimodal distribution in line with our experimental observations. **B:** Transition to stable reentry under I_{Na} and I_{NaL} reduction. Two typical examples of mVT transition are shown, depending on the initial condition: a stable spiral formation in the field of view **(top)** and a rotor moved out of the boundary while reentry formed around the perimeter of the cylinder geometry **(bottom).** Videos of transition to mVT are available in the Online Supplementary Materia1.